ANKLE

Normative rearfoot motion during barefoot and shod walking using biplane fluoroscopy

Kevin J. Campbell · Katharine J. Wilson ·
Robert F. LaPrade · Thomas O. Clanton

Abstract

Purpose The ankle rearfoot complex consists of the ankle and subtalar joints. This is an observational study on two test conditions of the rearfoot complex. Using high-speed biplane fluoroscopy, we present a method to measure rearfoot kinematics during normal gait and compare rearfoot kinematics between barefoot and shod gait.

Methods Six male subjects completed a walking trial while biplane fluoroscopy images were acquired during stance phase. Bone models of the calcaneus and tibia were reconstructed from computed tomography images and aligned with the biplane fluoroscopy images. An optimization algorithm was used to determine the three-dimensional position of the bones and calculate rearfoot kinematics.

Results Peak plantarflexion was higher (barefoot: 9.1°; 95 % CI 5.2:13.0; shod: 5.7°; 95 % CI 3.6:7.8; $p = 0.015$) and neutral plantar/dorsiflexion occurred later in the stance phase (barefoot: 31.1 %; 95 % CI 23.6:38.6; shod: 17.7 %; 95 % CI 14.4:21.0; $p = 0.019$) during barefoot walking compared to shod walking. An eversion peak of 8.7° (95 % CI 1.9:15.5) occurred at 27.8 % (95 % CI 18.4:37.2) of stance during barefoot walking, while during shod walking a brief inversion to 1.2° (95 % CI −2.1:4.5; $p = 0.021$) occurred earlier (11.5 % of stance; 95 % CI 0.2:22.8; $p = 0.008$) during stance phase. The tibia was internally rotated relative to the calcaneus throughout stance phase in both conditions (barefoot: 5.1° (95 % CI −1.4:11.6); shod: 3.6° (95 % CI −0.4:7.6); ns.).

Conclusions Biplane fluoroscopy can allow for detailed quantification of dynamic in vivo ankle kinematics during barefoot and shod walking conditions. This methodology could be used in the future to study hindfoot pathology after trauma, for congenital disease and after sports injuries such as instability.

Level of evidence II.

Keywords Gait · Rearfoot · Kinematics · Biplane fluoroscopy · Barefoot · Shod

K. J. Campbell · K. J. Wilson · R. F. LaPrade
Steadman Philippon Research Institute, 181 West Meadow
Drive, Suite 1000, Vail, CO 81657, USA
e-mail: drlaprade@sprivail.org

R. F. LaPrade · T. O. Clanton (✉)
The Steadman Clinic, 181 West Meadow Drive, Suite 1000,
Vail, CO 81657, USA
e-mail: tclanton@thesteadmanclinic.com

Introduction

The acceptation and differential diagnosis of ankle and subtalar joint instability remain a biomechanical and clinical conundrum. Patients with either ankle or subtalar instability commonly share the same subjective complaints and a characteristic symptomatology for either disorder has yet to be identified [2, 6, 17, 18]. The three-dimensional (3D) nature and dynamic interaction within the ankle rearfoot complex makes recognizing the underlying pathology extremely difficult. Furthermore, a reputable method of quantifying ankle rearfoot motion during both gait and dynamic weight-bearing activities has not been reported; however, this is of particular proclivity because it is during these manoeuvres when ankle and subtalar sprains and fractures transpire.

Motion sensor and optical marker systems have been used to measure foot and ankle kinematics to identify normal gait and adaptations after injury, surgery, or rehabilitation [8]. However, the 3D motion of many small bones of the foot may be at magnitudes less than the accuracy that can be obtained with motion capture. An

alternative and more accurate method of measuring joint kinematics is biplane fluoroscopy. This type of analysis has been used extensively for the shoulder [3, 11, 27] and knee [3, 13, 15, 32–34, 36] as a way of determining the movements of bones during dynamic activities with sub-millimetre and sub-degree accuracy [4, 12, 21, 25].

To date, only static biplane fluoroscopy studies have been employed to report weight-bearing positions of the ankle rearfoot complex [5, 9, 10, 19, 37]. Studies by Wainright et al. [37] and Caputo et al. [5] at Duke University used dual fluoroscopes to acquire a single pair of radiographs of the tibiotalar joint in a neutral position during static weight bearing of 25, 50, 75, and 100 % of body weight. Kozanek et al. [19] and de Asla et al. [9, 10] at Massachusetts General Hospital used dual fluoroscopes to acquire a single pair of radiographs of the ankle joint in three simulated static positions of gait; heel strike, mid-stance, and toe-off. To the authors' knowledge, no dynamic, weight bearing, in vivo fluoroscopy analyses, similar the methods proposed in the current study, have been conducted on the rearfoot or ankle and normative data does not exist for dynamic motions at these joints. In addition, a rigorous in vivo kinematic comparison of rearfoot motion between barefoot and shod walking has not been reported. This is of particular curiosity given previous reports that wearing shoes can have a profound effect on foot bone motion at the subtalar joint [29]. Biplane fluoroscopy could be used to understand all hindfoot pathology; including studying the effects of surgery such as fusion of the hindfoot, as well as pathology such as trauma, congenital disease such as flatfoot, cavus foot, and coalitions, and the effect of sports injuries and instability. The purposes of this study were to: (1) measure rearfoot kinematics during normal gait using high-speed biplane fluoroscopy; and (2) compare rearfoot kinematics between barefoot and shod gait. The null hypothesis was that healthy male subjects would exhibit the same peak plantarflexion and eversion angles during barefoot and shod walking.

Materials and methods

Six male recreational athletes [age 37.8 ± 8.6 years (mean $\pm$ standard deviation), height 1.82 ± 0.07 m, mass 75.7 ± 7.8 kg; BMI 22.9 ± 1.8 kg/m^2] with no history of ankle, knee, or hip injuries volunteered to participate in this study. All participants provided written informed consent approved by our Institutional Review Board prior to participation.

Collection of walking data

Upon arrival at the biomotion laboratory, participants completed a 5 min warm-up period consisting of barefoot walking. Subsequently, each participant walked along an elevated 10-m walkway while their right foot landed within the field of view of the biplane fluoroscopy system. Walking trial speeds were constrained via a metronome which set the foot fall cadence at 90 beats per minute. Participants completed five walking trials, and biplane fluoroscopy data were acquired during the fourth trial. In addition, a static standing trial of 0.1 s was collected during which each participant stood with their right foot within the biplane fluoroscopy field of view and their feet shoulder width apart. This procedure was repeated for shod walking while the participants wore a standardized running shoe without orthotic implants including medial posts or lateral crash pads (Saucony, Lexington, MA).

Biplane fluoroscopy system

The custom biplane fluoroscopy system was constructed from two commercially available BV Pulsera c-arms with 30-cm image intensifiers (Philips Medical Systems, Best, The Netherlands) which were modified under appropriate US Food and Drug Administration (FDA) guidelines. Two coupled high-speed digital cameras (resolution: $1,024 \times 1,024$; Phantom V5.1, Vision Research, Wayne, NJ), which were interfaced with the image intensifiers of the fluoroscopy systems, captured the dynamic radiographic images. Prior to data collection, the biplane fluoroscopy system was calibrated to determine the system configuration and correct for image distortion, as described in a previous study using this system [25]. Kinematic accuracies for tracking bones using our biplane fluoroscopy system have not been established for the foot, but have previously been reported for the knee [12]. In brief, the mean differences in joint kinematics between those determined by tantalum beads (gold standard) and those by tracking bone models were 0.2 mm [95 % confidence interval (95 % CI) $-0.4{:}0.8$ (lower bound : upper bound)], 0.1 mm (95 % CI $-0.5{:}0.7$), 0.1 mm (95 % CI $-0.4{:}0.6$) for medial/lateral, anterior/posterior and superior/inferior translations, respectively; and, $0.0°$ (95 % CI $-0.6{:}0.6$), $0.0°$ (95 % CI $-0.6{:}0.6$), $0.0°$ (95 % CI, $-0.7{:}0.7$) for flexion/extension, varus/valgus, and internal/external rotations, respectively. These translational and rotational accuracies are comparable to similar systems in the literature [1, 4, 21].

For each walking trial, biplane fluoroscopy data were collected for 1.0 s at 500 frames per second with a shutter speed of 1/2,000 s. The X-ray generators were operated in radiographic mode at 60 mA and 60 kV. In addition, a static computed tomography (CT) scan of the foot and tibia was obtained (slice thickness: 0.5 mm, resolution: 512×512 pixels) utilizing an Aquilion 64 scanner (Toshiba America Medical Systems, Tustin, CA) to obtain

Fig. 1 Coordinate system in a neutral position for the tibia and calcaneus
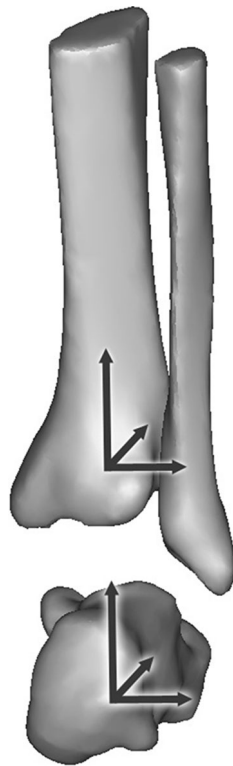
accurate 3D geometric descriptions of the bones in the ankle.

Data reduction

The 3D geometries of the calcaneus and tibia were extracted from the CT data using semi-automated commercial software (Mimics, Materialize, Inc., Ann Harbor, MI). Custom software written in MATLAB (The Mathworks, Natick, MA) was used to assign anatomical coordinate systems to the bones, as illustrated in Fig. 1. The tibial coordinate system was adapted from the International Society of Biomechanics (ISB) recommendations for the tibia/fibula coordinate system [38], as well a reference frame proposed by Ruff et al. [30], both which have been shown to have similar alignment [7]. The origin of the tibial coordinate system was positioned at the centre of the inferior surface of the distal tibia by determining the mid-points of the surface in the anteroposterior and mediolateral directions. The medial–lateral (ML) axis was assigned as a line from the mid-point on the medial side of the distal tibia surface to the mid-point on the lateral side, pointing laterally. The anterior-posterior (AP) axis was assigned perpendicular to the ML axis and a line connecting the origin to a point at the centre of the tibial shaft, pointing anteriorly. The superior-inferior (SI) axis was assigned perpendicular to the ML and AP axes, pointing superiorly. Since the ankle joint specimens were not in neutral stance during

the CT scans, a custom calcaneal coordinate system was adapted from the ISB recommendations for the calcaneus [38] to allow for anatomical positioning. The origin of the calcaneal coordinate system was positioned at the mid-point of three landmarks: inferior tuberosity, superior tuberosity, and the centre of the surface that articulated with the cuboid. The AP axis was assigned as a line between the mid-point of the inferior and superior tuberosities and the centre of the articulating surface with the cuboid, pointing anteriorly. The ML axis was assigned perpendicular to the AP axis and a line connecting the superior and inferior tuberosities, pointing laterally. The SI axis was assigned perpendicular to the AP and ML axes, pointing superiorly.

Ankle bone position and orientation was determined from the biplane fluoroscopy data using Model-based RSA software (RSAcore, Leiden, The Netherlands) [16]. Contours outlining the calcaneus and tibia bones were manually assigned in all radiographic frames. Subsequently, an automatic six degree-of-freedom optimization algorithm was used to align the tibial and calcaneal bone models with the contours selected in the biplane fluoroscopy images, and determine the 3D position and orientation of each bone (Fig. 2). The measurement accuracy of the bone model alignment was less than 0.5 mm for all frames.

Using the relative positions of the calcaneus and tibia in each frame, rearfoot kinematics were calculated with custom MATLAB software (The Mathworks, Natick, MA) using methods described by Grood and Suntay [14]. The translation and rotation of the calcaneus relative to the tibia were defined as rearfoot motion [24, 28, 39]. For each subject, the static standing joint angle was subtracted from all walking trials to normalize the data to a standardized ankle position. Plantar/dorsiflexion, eversion/inversion, and internal/external rotation were calculated for each barefoot and shod walking trial. The following parameters were also extracted from each individual trial: all three rotations at the time of heel strike, maximum plantarflexion, per cent stance phase at which the transition from plantarflexion to dorsiflexion occurred, maximum eversion during barefoot and maximum inversion during shod walking, and maximum internal tibia rotation.

Institutional review board approval

Approval from the Vail Valley Medical Center Institutional Review Board (IRB# 2009-08) was received prior to the data collection phase of this study.

Statistical analysis

Barefoot and shod kinematics were compared using paired t tests (IBM SPSS Statistics for Windows, Version 21.0.
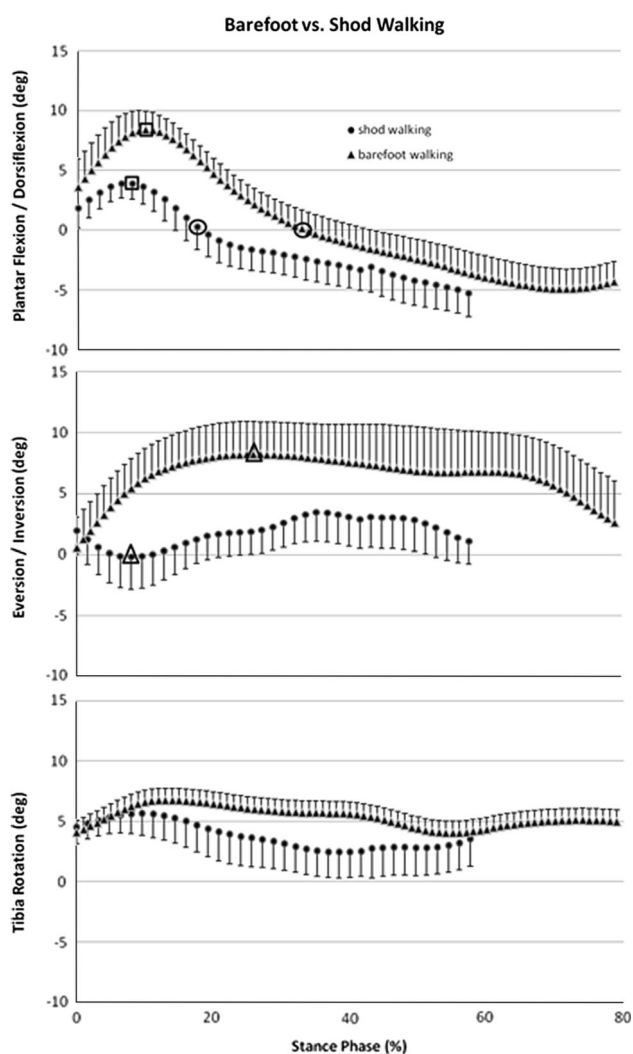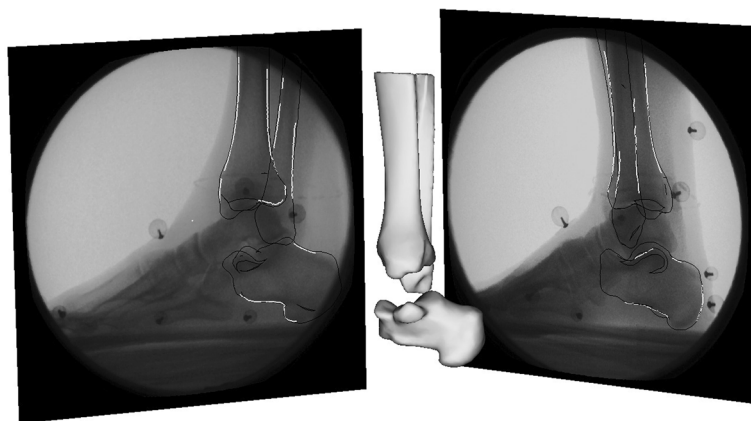
Fig. 3 Mean rearfoot kinematic profiles (±1 standard error) for the six subjects comparing barefoot and shod walking with regards to plantar flexion/dorsiflexion, eversion/eversion, and tibia internal/external rotation. Plantar flexion, eversion, and internal rotation are positive. *Squares* (peak plantar flexion), *circles* (neutral position), and *triangles* (peak eversion/inversion) indicate significant ($p < 0.050$) differences between barefoot and shod walking

IBM Corp., Armonk, NY) and significance threshold was set at $p < 0.05$.

Results

The mean profiles of the rearfoot kinematics of both barefoot and shod walking are displayed in Fig. 3. At least 80 % of stance phase was captured and processed for all six subjects for barefoot walking while at least 50 % was available for shod walking. The difference in the per cent of stance phase that could be captured was due to the increased height of the foot when wearing shoes which caused the tibia to rise out of the biplane capture volume earlier. The rearfoot was dorsiflexed during standing shod (5.3°; 95 % CI 1.1:9.5) compared to minimally plantar flexed during standing barefoot (0.2°; 95 % CI −5.4:5.8; $p = 0.001$). During the walking trials, the mean walking velocity was 1.4 m/s (95 % CI 1.2:1.6).

Plantarflexion/dorsiflexion

The foot contacted the ground in plantarflexion (barefoot: 3.6°; 95 % CI −2.4:9.6; shod: 2.4°; 95 % CI −1.5:6.3; ns.) and continued plantar flexing until peak plantarflexion, which occurred at approximately 10 % of stance (barefoot: 10.0 %; 95 % CI 6.3:13.7; shod: 7.9 %; 95 % CI 3.1:12.7; ns.). Peak plantarflexion was significantly higher for barefoot walking (9.1°; 95 % CI 5.2:13.0) compared to shod walking (5.7°; 95 % CI 3.6:7.8; $p = 0.015$). The foot then began to dorsiflex, reaching the standing neutral position significantly later at 31.1 % (95 % CI 23.6:38.6) of stance during barefoot walking compared to 17.7 % (95 % CI 14.4:21.0) of stance during shod walking ($p = 0.019$). Peak dorsiflexion of 4.9° (95 % CI 0.4:9.4) occurred at 66.3 % (95 % CI 51.5:81.1) of stance during barefoot walking, at which point the foot began to plantar flex again. Peak dorsiflexion was not reliably captured for

shod walking due to the limited field of view of the biplane fluoroscopy system in the raised position of the foot within the shoe.

Eversion/inversion

The rearfoot was on average everted during the capture period (barefoot: 5.7°; 95 % CI −1.5:12.9; shod: 1.7°; 95 % CI −2.2:5.6; ns.), contacting the ground in a position close to the standing neutral position (barefoot: 0.6°; 95 % CI, −5.8:7.0; shod: 1.5°; 95 % CI −3.4:6.4; ns.). During barefoot walking, the rearfoot everted to a maximum eversion of 8.7° (95 % CI 1.9:15.5), which occurred at 27.8 % (95 % CI 18.4:37.2) of stance, while during shod walking a brief inversion of 1.2° (95 % CI −2.1:4.5; $p = 0.021$) occurred significantly earlier (11.5 % of stance; 95 % CI 0.2:22.8; $p = 0.008$) during stance phase in most participants.

Internal/external tibial rotation

The tibia was on average internally rotated relative to the calcaneus throughout stance phase (barefoot: 5.1°; 95 % CI −1.4:11.6; shod: 3.6°; 95 % CI −0.4:7.6; ns.). Peak internal rotation of the tibia (barefoot: 7.5°; 95 % CI 0.4:14.6; shod: 8.1°; 95 % CI 4.3:11.9; ns.) occurred at approximately 15 % of stance (barefoot: 15.3 %; 95 % CI 5.0:25.6; shod: 13.3 %; 95 % CI 4.6:22.0; ns.), slightly before peak eversion.

Discussion

The most important result of the present study was the development of a novel modus to accurately quantify dynamic in vivo foot bone motion and presents an analysis of rearfoot motion during barefoot and shod walking. The most salient discoveries were that peak plantarflexion was significantly higher and neutral plantar/dorsiflexion occurred significantly later in the stance phase during barefoot walking as compared to shod walking. In addition, an eversion peak was demonstrated at the beginning of stance phase during barefoot walking, whereas an inversion peak was found during shod walking which occurred significantly earlier compared to the eversion peak in barefoot walking. The rearfoot was generally externally rotated for both conditions. The data reported herein highlight that rearfoot motion is different during barefoot and shod walking and helps establish baseline values for ankle rearfoot motion during walking. This information may prove beneficial for future researchers whom examine the changes that result from subtalar or ankle instability, degenerative arthritis, and joint fusion and could ultimately

provide valuable information related to total ankle arthroplasty.

Up to the present time, only static kinematics of the ankle joint complex have been reported using a biplane fluoroscopy system [5, 9, 10, 19, 37]. The static measurements in previous studies make it difficult to compare to the results of the present study because it is unclear exactly which points should be compared. For example, previous studies have not reported the load on the heel during a simulated heel strike or the percentage of the stance phase that it represents. Our data also demonstrate that the rearfoot angles change rapidly during initial weight acceptance and throughout the stance cycle. These transitions are not captured by a static analysis and are therefore unsuitable for a comprehensive analysis of ankle rearfoot motion.

The rearfoot motion during barefoot walking reported in the current study is somewhat similar to previously reported measures of rearfoot motion during barefoot walking using 3D video analysis and motion capture [20, 24]. Moseley et al. [24] also reported eversion of the calcaneus and internal rotation of the tibia throughout the first 80 % of stance phase. In contrast with the current work, Moseley and colleagues reported eversion and internal rotation to peak later in stance, while our data demonstrated that those values peaked near the beginning of stance phase. In addition, maximum reported eversion angles were higher in the current study compared to those reported by Moseley. Leardini et al. [20] also looked at bone motion between the tibia and calcaneus, reporting similar timing and magnitude of dorsiflexion and plantar flexion as the current work. Leardini et al. also reported similar timing of eversion; however, maximum eversion was lower for that study (3.0°) than the current work (8.7°) and they reported essentially no internal rotation of the tibia (maximum internal rotation in the current work: 7.5°). While similar results were found to studies using video analysis and motion capture, these systems are limited by lower accuracy due to skin motion artefact, joint centre estimations, and the 2D analysis of using video.

Current reports that compare 3D rearfoot kinematics between barefoot and shod walking are limited. In running, only one direct comparison could be discerned [31]. In this study, they reported that less inversion occurred at touchdown during barefoot running as compared to shod running. However, total eversion was reported to be similar between the two conditions. This is in contrast to our current study findings which demonstrated a significantly higher magnitude of eversion during barefoot walking as compared to shod walking. Both studies report that internal rotation was not affected by the shoe.

Furthermore, present descriptions of rearfoot kinematics are based on optical- or sensor-based systems. However, there are inherent errors in these systems, such as motion

artefacts caused by soft tissue movement during dynamic exercises and inconsistent marker placement over anatomical landmarks [23, 28, 35]. Markers attached to bone pins eliminate the inaccuracy due to soft tissue movement; yet, these methods are invasive and cause discomfort for subjects, potentially altering normal gait [22, 26, 28]. These limitations are largely overcome using a non-invasive highly accurate biplane fluoroscopy system as performed in this study. Additionally, biplane fluoroscopy can evaluate velocious motions such as running and jumping because it is capable of capturing up to 1,000 frames per second. This technology is also adept at assessing foot motion within the shoe and relative to the shoe, which have been extremely problematic in the past [28].

There are certain limitations with this study. First, only one trial per subject was collected and therefore intra-trial variability was not calculated or reported. Second, although tracking the calcaneus and tibia provided a strong representation of rearfoot motion, future studies need to explore the entire ankle joint complex, including the differences between subtalar and talocrural motion.

Conclusion

This study reports normative baseline values and significance differences in rearfoot motion during both barefoot and shod walking conditions. Clinicians should be mindful of the effect of wearing shoes on rearfoot motion when investigating subtalar pathology. This information will help future investigators quantify ankle and subtalar instability, the pathologic effects of degenerative arthritis and joint fusion, and may afford valuable information for the development of novel ankle replacement devices.

References

1. Anderst W, Zauel R, Bishop J, Demps E, Tashman S (2009) Validation of three-dimensional model-based tibio-femoral tracking during running. Med Eng Phys 31(1):10–16
2. Barg A, Tochigi Y, Amendola A, Phisitkul P, Hintermann B, Saltzman CL (2012) Subtalar instability: diagnosis and treatment. Foot Ankle Int 33(2):151–160
3. Bey MJ, Kline SK, Zauel R, Lock TR, Kolowich PA (2008) Measuring dynamic in vivo glenohumeral joint kinematics: technique and preliminary results. J Biomech 41(3):711–714
4. Bey MJ, Zauel R, Brock SK, Tashman S (2006) Validation of a new model-based tracking technique for measuring three-dimensional, in vivo glenohumeral joint kinematics. J Biomech Eng 128(4):604–609
5. Caputo AM, Lee JY, Spritzer CE, Easley ME, DeOrio JK, Nunley JA 2nd, DeFrate LE (2009) In vivo kinematics of the tibiotalar joint after lateral ankle instability. Am J Sports Med 37(11):2241–2248
6. Clanton TO (1989) Instability of the subtalar joint. Orthop Clin North Am 20(4):583–592
7. Conti G, Cristofolini L, Juszczyk M, Leardini A, Viceconti M (2008) Comparison of three standard anatomical reference frames for the tibia–fibula complex. J Biomech 41:3384–3389
8. Coughlan G, Caulfield B (2007) A 4-week neuromuscular training program and gait patterns at the ankle joint. J Athl Train 42(1):51–59
9. de Asla RJ, Kozanek M, Wan L, Rubash HE, Li G (2009) Function of anterior talofibular and calcaneofibular ligaments during in vivo motion of the ankle joint complex. J Orthop Surg Res 4:7
10. de Asla RJ, Wan L, Rubash HE, Li G (2006) Six DOF in vivo kinematics of the ankle joint complex: application of a combined dual-orthogonal fluoroscopic and magnetic resonance imaging technique. J Orthop Res 24(5):1019–1027
11. Giphart JE, Elser F, Dewing CB, Torry MR, Millett PJ (2012) The long head of the biceps tendon has minimal effect on in vivo glenohumeral kinematics: a biplane fluoroscopy study. Am J Sports Med 40(1):202–212
12. Giphart JE, Zirker CA, Myers CA, Pennington WW, LaPrade RF (2012) Accuracy of a contour-based biplane fluoroscopy technique for tracking knee joint kinematics of different speeds. J Biomech 45(16):2935–2938
13. Goyal K, Tashman S, Wang JH, Li K, Zhang X, Harner C (2012) In vivo analysis of the isolated posterior cruciate ligament-deficient knee during functional activities. Am J Sports Med 40(4):777–785
14. Grood ES, Suntay WJ (1983) A joint coordinate system for the clinical description of three-dimensional motions: application to the knee. J Biomech Eng 105(2):136–144
15. Kamath AF, Componovo R, Baldwin K, Israelite CL, Nelson CL (2009) Hip arthroscopy for labral tears: review of clinical outcomes with 4.8-year mean follow-up. Am J Sports Med 37(9):1721–1727
16. Kaptein BL, Valstar ER, Stoel BC, Rozing PM, Reiber JH (2003) A new model-based RSA method validated using CAD models and models from reversed engineering. J Biomech 36(6):873–882
17. Karlsson J, Eriksson BI, Renstrom PA (1997) Subtalar ankle instability. A review. Sports Med 24(5):337–346
18. Keefe DT, Haddad SL (2002) Subtalar instability. Etiology, diagnosis, and management. Foot Ankle Clin 7(3):577–609
19. Kozanek M, Rubash HE, Li G, de Asla RJ (2009) Effect of post-traumatic tibiotalar osteoarthritis on kinematics of the ankle joint complex. Foot Ankle Int 30(8):734–740
20. Leardini A, Benedetti MG, Berti L, Bettinelli D, Nativo R, Giannini S (2007) Rear-foot, mid-foot and fore-foot motion during the stance phase of gait. Gait Posture 25(3):453–462
21. Li G, Van de Velde SK, Bingham JT (2008) Validation of a non-invasive fluoroscopic imaging technique for the measurement of dynamic knee joint motion. J Biomech 41(7):1616–1622
22. Lundgren P, Nester C, Liu A, Arndt A, Jones R, Stacoff A, Wolf P, Lundberg A (2008) Invasive in vivo measurement of rear-, mid- and forefoot motion during walking. Gait Posture 28(1):93–100
23. Maslen BA, Ackland TR (1994) Radiographic study of skin displacement errors in the foot and ankle during standing. Clin Biomech 9(5):291–296

24. Moseley L, Smith R, Hunt A, Gant R (1996) Three-dimensional kinematics of the rearfoot during the stance phase of walking in normal young adult males. Clin Biomech (Bristol, Avon) 11(1):39–45

25. Myers CA, Torry MR, Peterson DS, Shelburne KB, Giphart JE, Krong JP, Woo SL, Steadman JR (2011) Measurements of tibiofemoral kinematics during soft and stiff drop landings using biplane fluoroscopy. Am J Sports Med 39(8):1714–1722

26. Nester C, Jones RK, Liu A, Howard D, Lundberg A, Arndt A, Lundgren P, Stacoff A, Wolf P (2007) Foot kinematics during walking measured using bone and surface mounted markers. J Biomech 40(15):3412–3423

27. Nishinaka N, Tsutsui H, Mihara K, Suzuki K, Makiuchi D, Kon Y, Wright TW, Moser MW, Gamada K, Sugimoto H, Banks SA (2008) Determination of in vivo glenohumeral translation using fluoroscopy and shape-matching techniques. J Shoulder Elbow Surg 17(2):319–322

28. Reinschmidt C, van Den Bogert AJ, Murphy N, Lundberg A, Nigg BM (1997) Tibiocalcaneal motion during running, measured with external and bone markers. Clin Biomech (Bristol, Avon) 12(1):8–16

29. Roberts S, Birch I, Otter S (2011) Comparison of ankle and subtalar joint complex range of motion during barefoot walking and walking in Masai Barefoot Technology sandals. J Foot Ankle Res 4:1

30. Ruff CB, Hayes WC (1983) Cross-sectional geometry of Pecos Pueblo femora and tibiae—a biomechanical investigation: I. Method and general patterns of variation. Am J Phys Anthropol 60(3):359–381

31. Stacoff A, Nigg BM, Reinschmidt C, van den Bogert AJ, Lundberg A (2000) Tibiocalcaneal kinematics of barefoot versus shod running. J Biomech 33(11):1387–1395

32. Tashman S, Collon D, Anderson K, Kolowich P, Anderst W (2004) Abnormal rotational knee motion during running after anterior cruciate ligament reconstruction. Am J Sports Med 32(4):975–983

33. Torry MR, Myers C, Shelburne KB, Peterson D, Giphart JE, Pennington WW, Krong JP, Woo SL, Steadman JR (2011) Relationship of knee shear force and extensor moment on knee translations in females performing drop landings: a biplane fluoroscopy study. Clin Biomech (Bristol, Avon) 26(10):1019–1024

34. Torry MR, Shelburne KB, Peterson DS, Giphart JE, Krong JP, Myers C, Steadman JR, Woo SL (2011) Knee kinematic profiles during drop landings: a biplane fluoroscopy study. Med Sci Sports Exerc 43(3):533–541

35. Tranberg R, Karlsson D (1998) The relative skin movement of the foot: a 2-D roentgen photogrammetry study. Clin Biomech (Bristol, Avon) 13(1):71–76

36. Van de Velde SK, Bingham JT, Gill TJ, Li G (2009) Analysis of tibiofemoral cartilage deformation in the posterior cruciate ligament-deficient knee. J Bone Joint Surg Am 91(1):167–175

37. Wainright WB, Spritzer CE, Lee JY, Easley ME, DeOrio JK, Nunley JA, DeFrate LE (2012) The effect of modified Brostrom–Gould repair for lateral ankle instability on in vivo tibiotalar kinematics. Am J Sports Med 40(9):2099–2104

38. Wu G, Siegler S, Allard P, Kirtley C, Leardini A, Rosenbaum D, Whittle M, D'Lima DD, Cristofolini L, Witte H, Schmid O, Stokes I (2002) ISB recommendation on definitions of joint coordinate system of various joints for the reporting of human joint motion-part I: ankle, hip, and spine. International Society of Biomechanics. J Biomech 35(4):543–548

39. Youberg LD, Cornwall MW, McPoil TG, Hannon PR (2005) The amount of rearfoot motion used during the stance phase of walking. J Am Podiatr Med Assoc 95(4):376–382